EFFECTS OF DISPLACEMENT RATES ON HYSTERESIS CURVES OF STEEL BEAMS AND COMPOSITE BEAMS

by

Koichi TAKANASHI[I)] and Kuniaki UDAGAWA[II)]

INTRODUCTION

Structural or member behavior under earthquake motion has been experimentally investigated by employing in most cases static monotonic and repeated tests for many years. Recently pseudo-dynamic response analyses of structures have been carried out by computer-load test apparatus hybrid on-line system[1)]. In these analyses, tests are also statically performed due to technical problems or for a measurement convenience. However, because structures respond to earthquakes dynamically, it is expected that a presumption of dynamic behavior based on static test data is not necessarily appropriate. Therefore, to explicate whether or not and how static test results are discrepant from dynamic test results makes it possible to confirm the reliability of those results and to ascertain relationship between data from the two tests.

There have been reports on comparison of static and dynamic hysteresis curves according to the above-mentioned view[2) - 7)]. Of them more have been concerned with studies of material properties rather than those of structural or member behavior. This paper deals with quasi-static and dynamic tests of realistic size steel beams and fully composite beams with steel deck subjected to monotonic and cyclic loadings, and compares differences of elastic-plastic behavior between the two tests. The specific objective is to experimentally investigate how the difference of displacement rates affects the following items:

1) Maximum moment capacity
2) Elastic stiffness and stiffness under unloading in plastic range
3) Deformation capacity and shape of hysteresis loop

TEST SPECIMENS

Five steel beams and five fully composite beams were tested. Considering the best-possible elimination of scale factor effects and an actuator capacity, half-size members were designed. A beam and a column stub of composite beam specimens were fabricated from a W 8 x 13 (H-202.9 x 101.6 x 5.84 x 6.48) section and a W 8 x 35 (H-206.2 x 203.7 x 7.87 x 12.57) section, respectively. Fig. 1 shows details of the specimens. The length of the specimen from the face of the column stub to a support point was 1.35 m long and represented the distance to the point of contraflexure. Full penetration butt weld was used for joining beam flanges to column flanges and

---

I) Professor, Institute of Industrial Science, University of Tokyo
II) Associate Professor, Department of Architecture, Tokyo Denki University

fillet weld for joining beam webs to the column flanges. The steel deck, dimension of which was D. H. -50 x 40 x 25 x 0.8, was oriented perpendicular to the steel beam and was split on the top flange of the steel beam.

A shear connection was designed according to ultimate strength design. The number and spacing of headed studs between the loading point and the face of the column stub were determined so as to resist the maximum horizontal shear. The 1,000 x 65 concrete slab was cast on the top flange of the steel beam. For slab reinforcement, 6 mm diameter steel bars were latticed at 17 mm deep from the slab surface with the spacing of 100 mm.

Steel beam specimens were identical with the composite beam specimens except for the concrete slab. The geometric properties of the steel elements of all the specimens are shown in Table 1. Table 2 shows the mechanical properties of flanges and webs of the steel elements of specimens. Each of these values was a mean for the results of coupon tension tests. The slab was made of lightweight concrete. Three cylinders were tested to obtain the strength of the concrete on the same day the composite beam specimens were tested. The mean strength of the concrete was 204.3 kg/cm^2. Table 1 also shows full plastic moments, ${}_sM_p$, of the steel beam specimens and the steel elements of the composite beam specimens as well as positive full plastic moment, ${}_cM_p$, and negative full plastic moment, ${}_cM_p'$, of the composite beam specimens. In these calculations the material properties of the steel and the concrete and actually measured thickness of the concrete slab were employed. But the width of the slab was made uniform to be 100 cm.

TEST SETUP

Fig. 2 shows the test setup schematically. A concentrated monotonic or cyclic load was applied to each beam specimen through the central column stub. The specimens were simply supported and were not allowed to move laterally at both ends. The column stub was also prevented from lateral movement by the supports, but its free rotation about the column axis was allowed. The top of the column stub was loaded by means of the servo-controlled hydraulic actuator which had a capacity of $\pm$20 tons dynamically and a maximum stroke of $\pm$150 mm.

LOADING PROGRAM AND DISPLACEMENT RATES

Monotonic and cyclic reversed loadings were given on both steel beams and composite beams. A sequence of the cyclic loadings was selected so that positive deflection amplitude may be equal to negative one. The magnitude of deflection amplitudes, δ, at the loading point was determined in such a way that beam rotation, θ, which was defined as δ/ℓ (ℓ: beam span between the support point and the face of the column stub) became the multiple of the rotation, ${}_s\theta_p$, which was defined as ${}_s\theta_p = {}_sM_p\ell^2/3EI$ (EI: flexural rigidity). The deflection amplitudes were progressively increased in the subsequent cyclic tests. The number of load reversals was four cycles in each deflection amplitude.

Three kinds of displacement rates were adopted, which were controlled at the loading point. Their nominal rates were 0.15 cm/sec for quasi-static tests and 15 cm/sec and 30 cm/sec for dynamic tests. Fig. 3 shows a time history of the displacement at the loading point. In the Figure, ${}_s\delta_p$ equals $\ell\,{}_s\theta_p$. Summarized in Table 3 is the details of loading program and the displacement rates of each specimen. In the Table, specimens S1 to S5 represent those of steel beams and specimens C1 to C5 those of composite beams.

MEASURING INSTRUMENTATION AND LOADING

Relative displacement between the loading point and the support point was measured by means of displacement transducers to determine the rotation, θ, of the beam specimens. The displacement transducers were mounted on the sides of the column stub. The applied load was measured by a load cell built into the actuator. Both loading and collecting test data were controlled by a minicomputer which was connected directly to the actuator system. The loading was controlled by the central displacement of the specimen as mentioned before. A displacement signal, which was programmed to generate a displacement-time relationship as shown in Fig. 3, was input into the actuator controller through a D/A converter under computer command. On the other hand, the data obtained from the experiment were stored in magnetic tape through A/D converters. This operation was also carried out by the same computer in parallel with the loading.

TEST RESULTS AND REMARKS

The moment-rotation relationships of the specimens are shown in Figs. 4 to 6. Of those figures, Fig. 4 shows the monotonic curves of the steel beams (S1 & S2) and the composite beams (C1 & C2). Figs. 5 and 6 indicate the hysteresis loops for cyclic tests of the steel beams (S3, S4 & S5) and the composite beams (C3, C4 & C5), respectively. Moment, M, is the applied beam moment at the face of the column stub and is normalized by the full plastic moment, ${}_sM_p$, of the steel element. On the other hand, beam rotation, θ, is normalized by the rotation, ${}_s\theta_p$.

Fig. 7 shows the relationship between the logarithm of the displacement rate, V, and maximum beam moment capacity, $m_{max} = M_{max}/{}_sM_p$, at the face of the column stub. The maximum beam moment capacities were defined as follows: in monotonic tests, it was the maximum moment capacity recorded under the loading; in cyclic reversed tests, it meant the positive and negative maximum moment capacity of the "stable" hysteresis loops obtained from the first cyclic loading in each test, for example, deflection amplitude of $2.33{}_s\theta_p$ in specimen S3 and deflection amplitude of $3.92{}_s\theta_p$ in specimen C3. Given in Fig. 8 is the relationship between the displacement rate, V, and the ratio of the maximum moment capacity, $M_{max}/{}_sM_p$, obtained from quasi-static tests and dynamic tests to the maximum moment capacity, $m_{max}^{static,\ mono} = M_{max}^{static,\ mono}/{}_sM_p$, from quasi-static monotonic tests. Fig. 9 shows the relationship between the displacement rate, V, and the ratio of the maximum moment capacity, $m_{max}^{dynamic} = M_{max}^{dynamic}/{}_sM_p$, in dynamic loadings to the maximum moment capacity, $m_{max}^{static} = M_{max}^{static}/{}_sM_p$, in quasi-static loadings. In these relationships between two maximum moment capacities of quasi-static and dynamic loadings, numerical ratios are given in Table 4.

The differences of elastic stiffness between quasi-static and dynamic loadings were not observed in both steel beams and composite beams. It was demonstrated by Fig. 4, which showed the moment-rotation curves of monotonic tests, and Figs. 5 and 6, which showed the hysteresis curves of the cyclic reversed tests. Figs. 5 and 6 also made it clear that there were no differences of stiffness under unloading in plastic range between the two loadings in both beams.

According to the conventional method in monotonic test and the method defined by authors in cyclic test before, the rotation capacity, R, of the beam specimens was calculated by $R = (\theta/{}_s\theta_p)_{max} - 1$[8), 9)]. In the equation, $(\theta/{}_s\theta_p)_{max}$ was defined as the beam rotation corresponding to the maximum moment in monotonic tests of steel beams, and in cyclic tests of steel beams and composite beams, defined as the maximum "stable" rotation amplitude,

beyond which beams failed. The rotation capacities are summarized in Table 3. In the Table, symbol, >, means that the rotation capacity is larger than that presented in the Table.

CONCLUSION

This experimental investigation was performed to make clear that how the hysteresis loops of the steel beams and the composite beams were affected by the displacement rates. The quasi-static tests and the dynamic tests were carried out for monotonic and cyclic loadings under the control of the displacement rate at the loading point. The nominal displacement rates were 0.15 cm/sec for the quasi-static test and 15 cm/sec and 30 cm/sec for the dynamic test. The following conclusions can be drawn from the test results in relation with the displacement rates:

1. Maximum moment capacities of steel beams and composite beams increase as a displacement rate increases. This was proved in both monotonic and cyclic reversed loadings. The largest increase in the maximum moment capacity of the dynamic loading from that of the quasi-static loading is about 20 % in the monotonic positive moment test of the composite beam. On the other hand, the smallest increase is about 5 to 8 % in the cyclic negative moment test of the composite beams. In case of the steel beams, increases are about 16 % in monotonic test and about 11 % in cyclic test. The details of the increase ratios are shown in Table 4.

2. The displacement rate does not affect the elastic stiffness for monotonic loadings nor the stiffness under unloading in plastic range for cyclic loadings regardless of steel beams and composite beams.

3. Though a detailed description was not made in this investigation, steel beams show a tendency to slightly increase rotation capacity as a displacement rate increases, but in case of composite beams there is no clear increase or decrease in rotation capacity even if a displacement rate increases.

ACKNOWLEDGMENTS

The authors wish to express their gratitude to the members of the working group of U.S.-Japan cooperative research program. The investigation was carried out as one of the support tests of pseudo-dynamic test of a full-size steel structure conducted by U.S.-Japan cooperative research program utilizing large-scale testing facilities. The experiment was supported by the Kozai Club and Building Constructors Society.

REFERENCES

1. Takanashi, K., Udagawa, K., and Tanaka, H., "Earthquake Response Analysis of Steel Frames by Computer-Actuator On-Line System," Proc. of the Fifth Japan Earthquake Engineering Symposium, 1978.
2. Hanson, R.D., "Comparison of Static and Dynamic Hysteresis Curves," Proc. of the ASCE, Jour. of the Engineering Mechanics Division, Vol. 92, October 1966

3. Almuti, A.M., and Hanson, R.D., "Static and Dynamic Cyclic Yielding of Steel Beams," Proc. of the ASCE, Jour. of the Structural Division, Vol. 99, June 1973.
4. Mukudai, Y., and Matsuo, A., "Local Buckling of Flange and Hysteresis Characteristics of Beams under Static and Dynamic Cyclic Loadings," Proc. of the Annual Convention of the Architectural Institute of Japan, October 1975 (in Japanese).
5. Wakabayashi, M., Nakamura, T., Yoshida, N., and Iwai, S., "Effect of Strain Rate on Stress-Strain Relationships of Concrete and Steel," Proc. of the Fifth Japan Earthquake Engineering Symposium, 1978.
6. Fujimoto, M., and Nanba, T., "Effect of Deformation Rate on Deformation Capacity of Steel Elements," Proc. of the Annual Convention of the Architectural Institute of Japan, September 1980 (in Japanese).
7. Aoki, H., Kato, B., Nanba, T., and Satoh, N., "Influences of Test Temperature and Load Velocity on Ultimate Strength and Deformation of Notched Steel Elements," Transaction of the Architectural Institute of Japan, No. 322 December 1982 (in Japanese).
8. Udagawa, K., Takanashi, K., and Tanaka, H., "Restoring Force Characteristics of H-Shaped Steel Beams under Cyclic and Reversed Loadings," Transaction of the Architectural Institute of Japan, No. 264, February 1978 (in Japanese).
9. Naka, T., Umino, S., Udagawa, K., and Mimura, H., "Experiments on Restoring Force Characteristics of Composite Beams," Proc. of the Annual Convention of the Architectural Institute of Japan, October 1982 (in Japanese).

Table 1 Summary of Specimens

Specimen	B/t_f	H/t_w	$l/_s r_y$	${}_sM_p$ (t·cm)	${}_cM_p$ (t·cm)	${}_cM_p'$ (t·cm)
S 1	15.0	35.8	61.9	575.9	—	—
S 2	15.1	35.8	61.3	575.1	—	—
S 3	15.0	35.9	61.3	573.8	—	—
S 4	15.0	35.6	61.4	577.0	—	—
S 5	15.1	35.7	61.3	575.6	—	—
C 1	15.0	35.7	61.4	571.2	1070.5	709.4
C 2	15.0	35.6	61.3	569.6	1069.7	707.7
C 3	15.0	35.6	61.3	569.9	1089.3	709.4
C 4	15.0	35.6	61.4	573.3	1088.7	712.9
C 5	15.0	35.2	61.6	571.1	1102.7	711.7

Table 2 Material Properties of Steels

Specimen	σ_y(t/cm^2)	σ_{max}(t/cm^2)	ε_{st}(x10^{-3})	E_{st}(t/cm^2)	ε_B(%)
Flange	2.82	4.18	18.9	36.1	27
Web	3.72	4.74	18.0	32.5	23

Table 3 Summary of Test Results

Specimen	Loading Condition	Displacement Amplitude($s\theta_p$)	No.of Cycle	Displacement Rate(cm/sec)	Rotation Capacity
S1	Monotonic			0.14	5.25
S2	Monotonic			30.3	7.0
S3	Cyclic	2.33	4	0.14	1.87
		2.87	4	0.14	
		2.98	4	29.8	
		2.87	4	0.14	
		3.30	4	0.14	
S4	Cyclic	2.37	4	14.3	> 2.43
		2.92	4	14.6	
		3.43	4	14.7	
		3.99	4	15.0	
S5	Cyclic	2.35	4	28.2	> 2.38
		2.93	4	29.3	
		3.38	4	28.9	
C1	Monotonic			0.15	
C2	Monotonic			30.2	
C3	Cyclic	3.92	4	0.15	2.92
		4.43	4	0.15	
C4	Cyclic	3.98	4	14.9	2.98
		4.57	4	15.2	
C5	Cyclic	4.02	4	30.2	3.02
		4.68	4	31.2	

Table 4 Moment Increase Ratio of Dynamic Loading to Quasi-Static Loading

Specimen	Loading		Nominal Displacement Rate (cm/sec)		
			0.15	15	30
Steel Beam	Monotonic		1	—	1.16
	Cyclic		1	1.11	1.11
Composite Beam	Monotonic Positive Moment		1	1.15	1.20
	Cyclic	Positive Moment	1	1.07	1.10
		Negative Moment	1	1.05	1.08

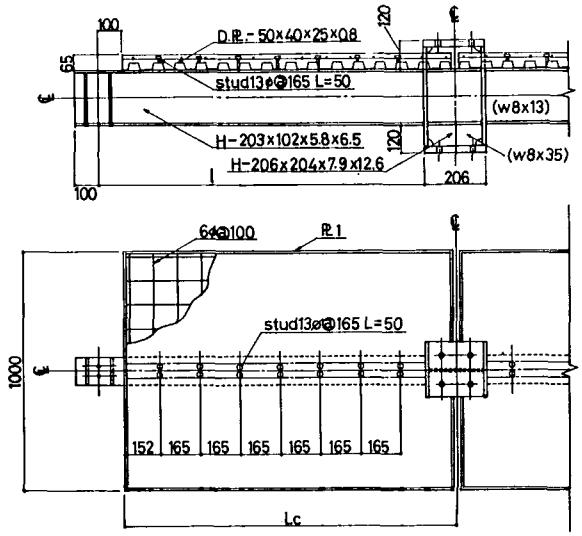

Fig.1 Test Specimen of Composite Beam

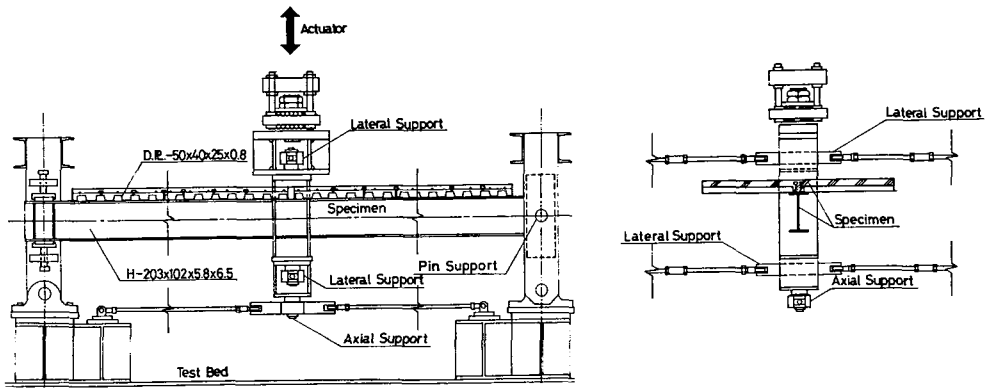

Fig.2 General View of Test Setup

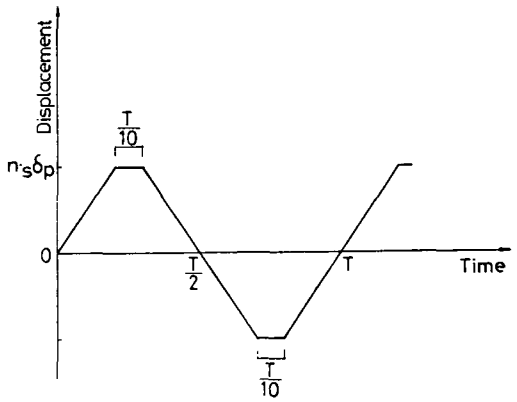

Fig.3 Time History of Applied Displacement

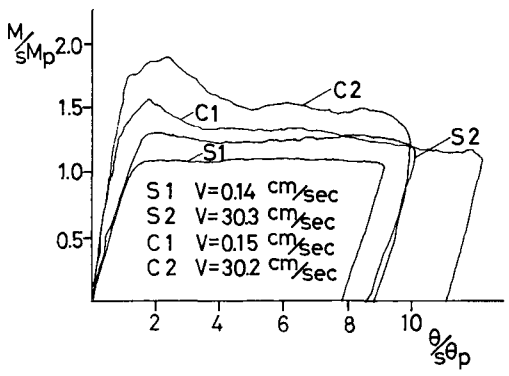

Fig.4 Moment and Rotation Curves

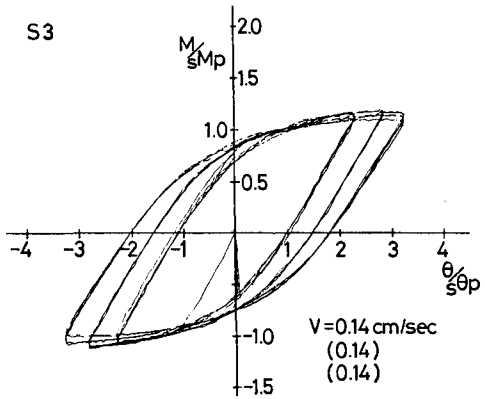

(a) Specimen S3

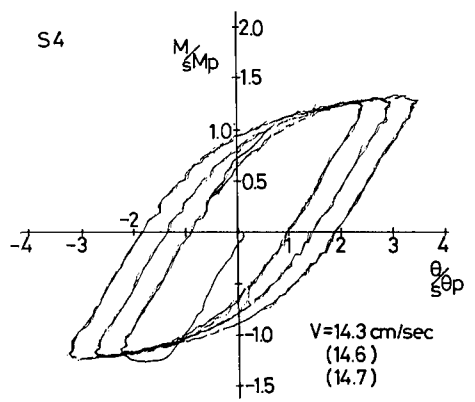

(b) Specimen S4

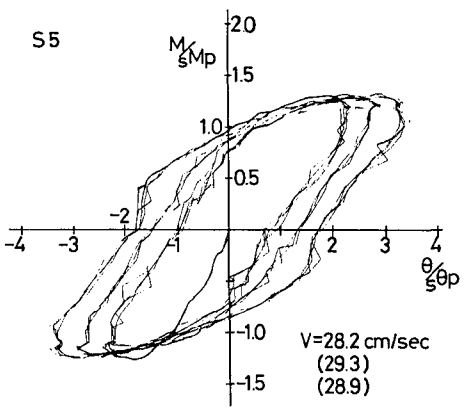

(c) Specimen S5

Fig.5 Hysteresis Loops of Steel Beams

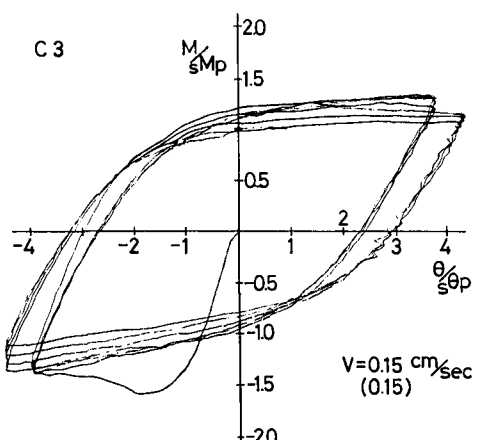

(a) Specimen C3

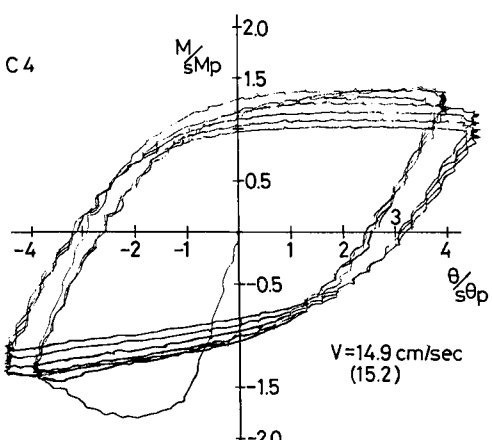

(b) Specimen C4

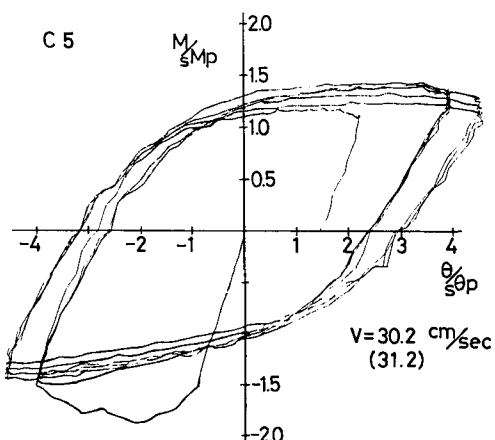

(c) Specimen C5

Fig.6 Hysteresis Loops of Composite Beams

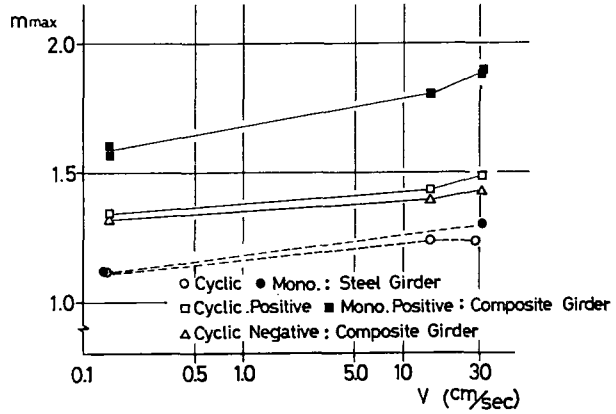

Fig.7 Displacement Rate and Maximum Moment

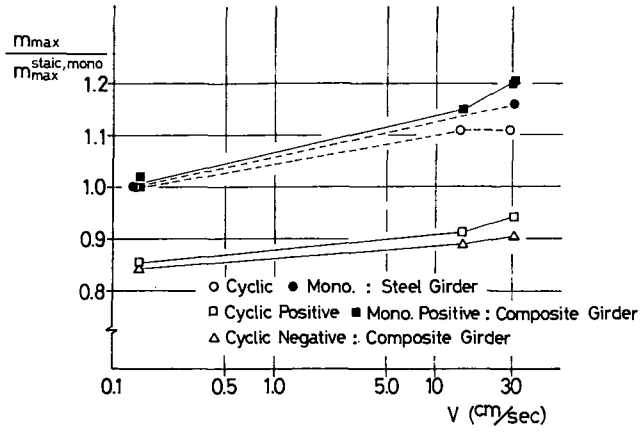

Fig.8 Displacement Rate and Ratio of Maximum Moment to Maximum Moment in Quasi-Static Monotonic Tests

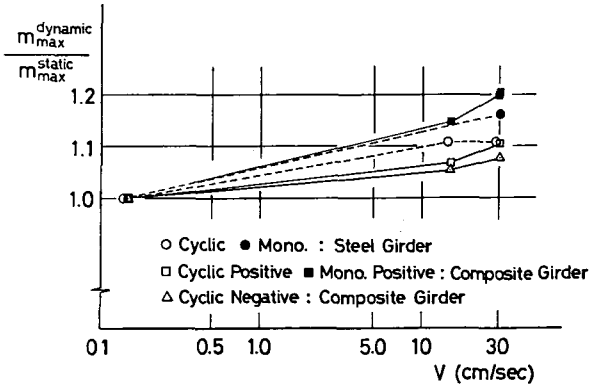

Fig.9 Displacement Rate and Ratio of Maximum Moment in Dynamic Tests to Maximum Moment in Quasi-Static Tests